Journal of Peptide Science
J. Peptide Sci. **11**: 289–302 (2005)
Published online 5 November 2004 in Wiley InterScience (www.interscience.wiley.com). DOI: 10.1002/psc.627

JOURNAL OF PEPTIDE SCIENCE

Complete structure determination of *N*-acetyl-D-galactosamine-binding mistletoe lectin-3 from *Viscum album L. album*

ROLAND WACKER, STANKA STOEVA, CHRISTIAN BETZEL and WOLFGANG VOELTER*

Abteilung für Physikalische Biochemie des Physiologisch-chemischen Instituts der Universität Tübingen, Hoppe-Seyler-Str. 4, D-72076 Tübingen, Germany

Received 19 August 2004; Accepted 29 August 2004

Abstract: The primary structure of the B chain of the *N*-acetyl-D-galactosamine-recognizing mistletoe lectin-3 (ML-3B) has been deduced from proteolytic digest peptides of the purified glycoprotein, their HPLC-separation and Edman degradation and confirmation of the peptide sequences by MALDI-MS. ML-3B consists of 262 amino acid residues including 10 cysteine moieties. The structure and linkage of the carbohydrate side chains, connected to two N-glycosylation sites at positions Asn^{95} and Asn^{135} of the lectin, were determined by a combination of glycosidase treatment and MALDI-MS of corresponding glycopeptide fragments. The sequence alignment reveals a high homology with other B chains of type-II RIPs, although there are remarkable differences in the D-galactose-specific mistletoe lectin-1B chain. The recently published primary structure of the mistletoe lectin-3A chain [1] and the now available primary sequence of the 3B chain allowed the construction of a preliminary homology model of ML-3. The model demonstrates, unequivocally, that ML-3 is a member of the type-II RIP family with rigid conservation of the enzymatic active site of the A chain and an identical overall protein fold. Specific amino acid residue exchanges and the different glycosylation pattern in comparison with ML-1 are discussed and related to the properties of the two glycoproteins. The knowledge of the complete primary structure of mistletoe lectin-3 is a major contribution towards more insight into the mechanism of the biological activity of commercial mistletoe preparations.

Keywords: lectins; mistletoe; glycosylation sites; ribosome-inactivating proteins

INTRODUCTION

Extracts of the European mistletoe (*Viscum album L. ssp. album*) are commonly used as immunomodulating agents in human cancer treatment. The patient receiving mistletoe therapy is supposed to benefit from an improved non-specific immune defence, caused by an increased number and activity of T-lymphocytes and natural killer (NK) cells [2,3], an enhancement of the phagocytic activity of granulocytes [4] and the induction of cytokine secretion [5–7]. It could be demonstrated that a group of glycoproteins is responsible for the immunomodulatory potency of mistletoe extracts [8]. These so-called mistletoe lectins are typical representatives of ribosome-inactivating proteins (RIP) of type-II [9], commonly found in the plant kingdom. Besides their immunomodulatory activity, it could be demonstrated that mistletoe lectins are strong cytotoxic agents *in vitro* [10–13] and are able to induce apoptosis to cultured human cells [6,14,15]. They are constituted of two different subunits, the cytotoxic A chain and the carbohydrate-binding B chain, linked by a single disulfide bond. In mistletoe plants three different type-II RIPs were identified, differing in their monosaccharide specificity and molecular weight: mistletoe lectin-1 binds to D-galactose, mistletoe lectin-3 to *N*-acetylgalactosamine and mistletoe lectin-2 recognizes both monosaccharides [16–18].

Recently, the primary structure of ML-1 was determined by Edman degradation [19,20] and DNA sequencing [21,22]. Moreover, the three-dimensional structure of ML-1 could be established by x-ray diffraction analysis [23]. From these results it became obvious that ML-1A inhibits protein synthesis by depurinating a single adenine of the ribosomal RNA by the same mechanism as supposed for ricin [10]. The B chain of ML-1, supposed to be a product of a series of gene duplications, consists of six homologous subdomains $\alpha 1$, $\alpha 2$, $\beta 1$, $\beta 2$, $\gamma 1$ and $\gamma 2$, originating from an ancient galactose-binding peptide [24,25]. Only the $\alpha 1$ and the $\gamma 2$ subdomains retained their ability to bind galactose. The interaction of the carbohydrate-recognizing B chain with surface receptors of the target cell containing terminal galactose structures is essential to enable the endocytotic uptake of the cytotoxic A chain and inhibition of protein synthesis [15]. The different carbohydrate specificity of the mistletoe

Abbreviations: AC, affinity chromatography; ML, mistletoe lectin; PMP, 1-phenyl-3-methyl-5-pyrazolone; PNGaseF, peptide-N-(acetyl-β-glucosaminyl)-asparaginamidase; RCA, *Ricinus communis* agglutinin; RIP, ribosome-inactivating protein; SNAI', *Sambucus nigra* agglutinin I'; TFA, trifluoroacetic acid; Tris, tris(hydroxymethyl)aminomethane.

*Correspondence to: Professor Wolfgang Voelter, Abteilung für Physikalische Biochemie der Universität Tübingen, Hoppe-Seyler-Str. 4, D-72076 Tübingen, Germany; e-mail: wolfgang.voelter@uni-tuebingen.de

isolectins makes them potentially useful as effective and selective anti-cancer drugs. Numerous studies of the biological activity of mistletoe isolectins indicated a differently pronounced cytotoxicity as a consequence thereof [9,11,12]. From DNA sequencing, so far only one gene could be detected and the sequence data [21] were not in complete coincidence with the primary structure of ML-1 identified by protein sequencing [19,20]. To date, the origin, different carbohydrate specificity and molecular structure of the different isoforms remain unclear. It was proposed that ML-2 and ML-3 were isolation artefacts or products of mistletoe lectin-1 that undergo posttranslational modifications or degradation steps [21,22].

Without any further characterization of the isolectins ML-2 and ML-3, a deeper insight into the structure-function relationship on a molecular basis and the efficient development of chimeric drugs or analytical procedures for the standardization of mistletoe extracts will not be possible. Therefore it was decided to determine the primary structure and the glycosylation profile of the mistletoe lectin-3B chain from the isolated protein.

MATERIALS AND METHODS

Materials

Trypsin, chymotrypsin and peptide-N-glycosidase F (rec. *E. coli*) were purchased from Roche Diagnostics GmbH, Mannheim, Germany. α1–2,3,6-, α1–2,3- and α1-2-mannosidase were obtained from Calbiochem, Schwalbach, Germany. SP-Sephadex and Sepharose 4B were purchased from Amersham Bioscience, Freiburg, Germany. The 10 kDa ladder protein mixture was obtained from Gibco BRL, Eggenstein, Germany. All reagents for peptide sequencing were from the original supplier Applied Biosystems, Warrington, UK. All other chemicals and reagents were supplied in p. a. quality from Merck, Darmstadt, Germany or Sigma-Aldrich, Taufkirchen, Germany.

Methods

Preparation of the affinity gel. 200 ml Sepharose 4B was washed two times with 400 ml 0.5 M sodium carbonate, pH 11.0 and suspended in 200 ml of the same buffer. Over a time period of 60 min 24 ml of divinylsulfone was added dropwise in the dark. After 60 min of continuous stirring, the liquid was exchanged by 350 ml of 0.5 M sodium carbonate, pH 10.0 and 20 g of lactose was added. After stirring for 12 h in the dark, the reaction was stopped by the addition of 200 ml 0.5 M sodium carbonate, pH 8.5, containing 8 ml 2-mercaptoethanol, and stirring for 4 h. Finally, the gel was washed with phosphate-buffered saline and stored in 20% ethanol.

Isolation of mistletoe lectins. 500 g fresh mistletoe leaves were frozen in liquid nitrogen and ground with a Waring blendor. The plant powder was suspended in 1000 ml water and stirred at 4 °C for 12 h. After filtration through a canvas cloth, the pH of the extract was adjusted to 4.75 with acetic acid under stirring. The resulting precipitate was removed by centrifugation at 6000 ×g and 50 g swollen SP-Sephadex C-25 was added to the supernatant. After stirring for 2 h at 4 °C, the ion exchanger was removed with a frit and washed with 50 mM sodium acetate buffer, pH 4.75, until the effluent was colourless. After filling the gel into a column (16 × 80 mm), the washing step was continued until the eluate was free of protein. The absorbed proteins were eluted with 0.1 M Tris/HCl, 0.5 M NaCl, pH 8.0 in a volume of about 200 ml.

The protein concentrate was loaded onto an affinity column (50 × 100 mm), filled with lactosyl-sepharose and the unbound protein fraction was eluted with 0.1 M Tris/HCl, 0.5 M NaCl, pH 8.0. A fraction containing ML-3 besides ML-1 was desorbed by adding galactose to the buffer to a final concentration of 20 mM. By increasing the galactose concentration in the buffer to 0.1 M, a second fraction mainly containing ML-1 could be obtained. The proteins were precipitated with 50% (w/w) ammonium sulphate and removed by centrifugation at 4000 ×g at 4 °C for 60 min. The supernatant was discarded, the pellet dissolved in 15 mM sodium citrate, pH 4.2, and the isolectins separated by ion exchange chromatography on a Mono S HR 5/5 column (Pharmacia Biotech AB, Uppsala, Sweden) with a linear sodium chloride gradient from 0 to 0.6 M in 10 column volumes (buffer A: 15 mM sodium citrate, pH 4.2, buffer B: 1 M sodium chloride in buffer A; flow rate: 1.0 ml/min; detection wavelength: 280 nm). A mistletoe lectin-3-containing fraction could be collected manually at a sodium chloride concentration of 0.32 M, while the ML-1 desorbed in two isoforms at a concentration of 0.41 M sodium chloride, respectively. The proteins were again recovered by ammonium sulphate precipitation (50% w/w) and stored as suspensions at 4 °C. The purity of the preparations was checked by SDS gel electrophoresis and the ion exchange chromatography step repeated, if necessary.

SDS gel electrophoresis. SDS polyacrylamide gel electrophoresis of the purified proteins was carried out according to Laemmli *et al.* [26] using a 10 × 10 cm vertical system (Owl, Portsmouth/NH, USA) and a constant current voltage of 120 V for 3 h. Proteins were stained with Coomassie blue G 250. Calibration of protein bands was achieved by using a 10 kDa protein ladder standard, supplied by Gibco BRL, Eggenstein, Germany.

Haemagglutination assay. Agglutination assays were carried out in 96-well micro titer plates in a final volume of 100 µl. To 50 µl of a twofold serial dilution with PBS of the lectin sample solution, 50 µl of a 4% erythrocyte suspension (human B-type, Rh. negative) in PBS was added. After an incubation time of 1 h, the mixtures were stirred with a pipette tip and the haemagglutination activity was determined visually. Haemagglutination units were defined as the maximum dilution factor of a sample solution in which unequivocal agglutination was detectable.

Reduction and alkylation of cysteine residues. Reduction of lyophilized mistletoe lectin-3 (5 mg) with 2-mercaptoethanol (10 µl) was carried out in a final volume of 1 ml 0.1 M Tris/HCl, 8 M urea, pH 7.75, at room temperature for 14 h in the dark. Then, 15 µl of 4-vinylpyridine was added and the reaction mixture stirred in the dark for 4 h [28]. The alkylated ML-3 was

desalted by dialysis against distilled water (Visking dialysis tubing 36/32, Serva, Heidelberg, Germany) and lyophilized.

Enzymatic digestion. Chymotrypsin digestion of ML-3 (2.2 mg) was performed at 25 °C and for 3 h in 333 µl 0.1 M Tris/HCl, 6 M guanidine/HCl, 61 mM $CaCl_2$, pH 7.8, containing 50 µg protease. The tryptic digestion of ML-3 (5.0 mg) was carried out using 4 ml 0.2 M Tris/HCl, 10% CH_3CN, pH 8.5, and 250 µg trypsin added in five portions over a time period of 18 h at 37 °C under stirring.

Fractionation of peptides. The enzymatic digest was acidified with TFA until a pH of 3 was obtained and centrifuged from insoluble material. The soluble peptides from the chymotryptic digest were fractionated via RP-HPLC on a Gromsil C-18 column (100-5 ODS, 4.6 × 250 mm) with a linear gradient of acetonitrile, containing 0.1% (v/v) TFA at a flow rate of 1 ml/min. For the tryptic digest peptides, a Nucleosil 100-7 RP 18 column (10 × 250 mm; Machery Nagel, Düren, Germany) was used under the same conditions as mentioned above. The eluted peptides were detected by UV absorbance at 220 nm, collected manually and recovered by lyophilization. The insoluble peptides precipitating during the acidification step after proteolysis were separated by centrifugation, reconstituted with concentrated formic acid, immediately diluted to 10% formic acid with distilled water and filtered through a microconcentrator (Nanosep Microconcentrator 10 kDa; Pall, Northborough, MA, USA) with a 10 kDa molecular weight cut-off membrane. The filtered peptides were separated by RP-HPLC on a Parcosil ProRP 300 C4 column (Serva, Heidelberg, Germany; dimensions: 4.6 × 100 mm) with a linear gradient of acetonitrile, containing 0.1% (v/v) TFA at a flow rate of 1 ml/min. The fractions were lyophilized and reconstituted with 50 µl 0.1% TFA.

Sequence analysis. Automated Edman degradation was performed using an Applied Biosystems pulsed liquid sequencer model 473A (Applied Biosystems, Weiterstadt, Germany) with online analysis of the phenylthiohydantoin (PTH) derivatives according to the manufacturer's operation instructions.

Mass spectrometric analysis. Matrix-assisted laser desorption ionization (MALDI) mass spectra were obtained from the isolated peptides and proteins using a Kratos Kompact MALDI II instrument (Shimadzu, Torrance/CA, USA). The matrix used for peptides was a solution of 200 mg α-cyano-4-hydroxycinnamic acid and 50 mg nitrocellulose in a 1 : 1 mixture of acetone and isopropanol [28]. For mass determination of proteins, a solution of 1 mg/ml trans-ferrulic acid in 30% acetonitrile, 0.1% TFA, in water was chosen.

Monosaccharide composition analysis. The monosaccharide composition of ML-3-linked oligosaccharides was investigated by a HPLC-based approach according to references [29] and [30]. In brief, 50 to 250 µg of the purified lectin sample was hydrolysed with 1 ml 4 M TFA at 121 °C in a glass ampoule for 2 h. After lyophilization of the sample, the residue was treated with 50 µl of a 0.3 M sodium hydroxide solution and 50 µl of 0.5 M 1-phenyl-3-methyl-5-pyrazolone (PMP) in methanol. The mixture was then heated for 2 h at 70 °C. After cooling to room temperature, 50 µl 0.3 M HCl was added, the sample agitated and centrifuged. Excess reagent was removed by extraction with 3 × 500 µl chloroform and the remaining aqueous phase analysed after filtration by RP-HPLC using a Hypersil HyPurity Elite C18-5 column (4.6 × 250 mm, ThermoQuest, Runcorn, GB). The chromatographic conditions were as follows: buffer A: 0.1 M ammonium acetate, 10% (v/v) CH_3CN, pH 5.5; buffer B: 0.1 M ammonium acetate, 25% (v/v) CH_3CN, pH 5.5; gradient elution: 0–5 min: 45% B, 5–50 min: 45%–100% B, 50–90 min: 100% B; flow rate 1 ml/min; detection wavelength: 245 nm.

The individual amount of each reducing monosaccharide residue was calculated by comparing peak areas with values from an external monosaccharide standard calibration curve, based on 0.1 to 20 nmol samples of the following monosaccharides: *N*-acetyl-D-galactosamine, *N*-acetyl-D-glucosamine, D-mannose, D-galactose, D-glucose, L-fucose and D-xylose.

Glycan structure analysis of glycopeptides from ML-3B. Aliquots of glycopeptide fractions received from the protease cleavage were lyophilized, reconstituted in 50 µl 0.1% TFA in water and digested with exoglycosidases or peptide-N-glycosidase F according to the following procedures.

Peptide-N-glycosidase F (*rec. E. coli*): 4 µl of a solution of 250 mU/µl in 0.1 M sodium phosphate, pH 7.2, was mixed with a 3 µl sample solution and 1 µl 0.1 M Tris/HCl, pH 8.0.

α1-2,3,6-Mannosidase (*Jack Bean*): 1 µl of a solution of 10 mU/µl in 20 mM Tris/HCl, 20 mM sodium chloride, pH 7.5, was mixed with a 2 µl sample solution and then 6 µl of 0.05 M sodium acetate, 2 µM zinc chloride, pH 5.0, were added.

α1-2,3-Mannosidase (*rec. E. coli*): 2 µl of a 2 U/µl solution in 20 mM Tris/HCl, 20 mM sodium chloride, pH 7.5, was added to a mixture of 4 µl sample solution and 2 µl of a solution of 0.05 M sodium citrate, 5 mM calcium chloride, 0.1% BSA, pH 6.0.

α1-2-Mannosidase (*Aspergillus satoi*): 2 µl of a 1 µU/µl solution in 0.1 M sodium acetate, pH 5.0, was mixed with a 2 µl sample solution and then 5 µl of 0.1 M sodium acetate, pH 5.0, were added.

The samples were incubated at 37 °C for 24 h and 1 µl aliquots were examined by MALDI-MS after 2 and 24 h using a nitrocellulose-containing α-cyano-4-hydroxy-cinnamic acid matrix.

RESULTS

Isolation and Purification of Mistletoe Lectin-3

ML-3 was isolated according to the method of Eifler *et al.* [18] (Figure 1). The ML-3-containing protein fraction, collected by affinity chromatography, was further purified by ion exchange chromatography with a MonoS© HR 5/5 column (Figure 2). The ML-3-containing fraction contained considerable amounts of ML-1. The amounts of ML-3, isolated from 100 g fresh harvested mistletoe leaves, varied from 0.1 mg to 0.5 mg and thus was equivalent to about 5% of the corresponding amount of ML-1.

The activity of the lectin was checked by the haemagglutination assay, resulting in a maximum haemagglutination titer of 64 for a 1 mg/ml lectin concentration (human B-type Rh. neg.). In the same assay, for ML-1 a value of 256 units was determined,

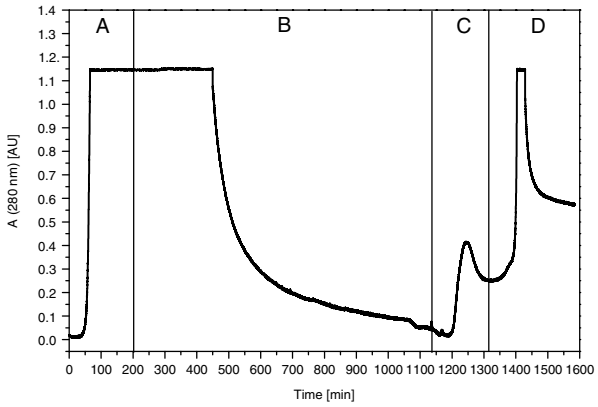

Figure 1 Isolation of ML-3 and ML-1 from mistletoe extract by affinity chromatography on a divinylsulfone-activated lactosyl-Sepharose 4B column (50 × 120 mm). The column was loaded with 400 ml of protein concentrate (A) and unbound proteins were removed with 0.1 M Tris/HCl, 0.5 M NaCl, pH 8.0 (B). The ML-3-containing fraction was eluted by adding 20 mM galactose to the buffer (C). A second, mainly ML-1-containing fraction, was collected by increasing the concentration of galactose to 0.1 M (D). Flow rate: 2 ml/min, detection wavelength: 280 nm.

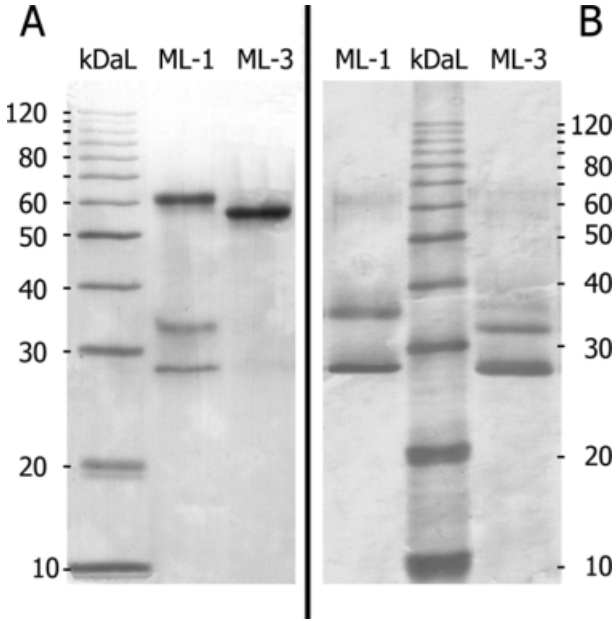

Figure 3 SDS-PAGE of ML-3 and ML-1, A (under non-reducing conditions, without β-mercaptoethanol) and B (under reducing conditions in the presence of β-mercaptoethanol) using a 12% gel and 10 µg sample. Electrophoresis was performed at 110 V and the gel stained with Coomassie brilliant blue R250. As molecular weight marker a 10 kDa protein ladder (kDaL, GibcoBRL, Germany) was used.

demonstrating ML-1 to be a stronger agglutinating agent compared with ML-3, referring to human B-type erythrocytes.

Molecular Weight Determination of Mistletoe Lectin-3

The purity of the protein was checked by SDS gel electrophoresis (Figure 3) and the molecular weight of ML-3 was estimated to be 58 000 Da. For ML-1, a molecular weight of 61 000 was determined. In the presence of β-mercaptoethanol (Figure 3A) two bands originating from the heterodimeric lectins were

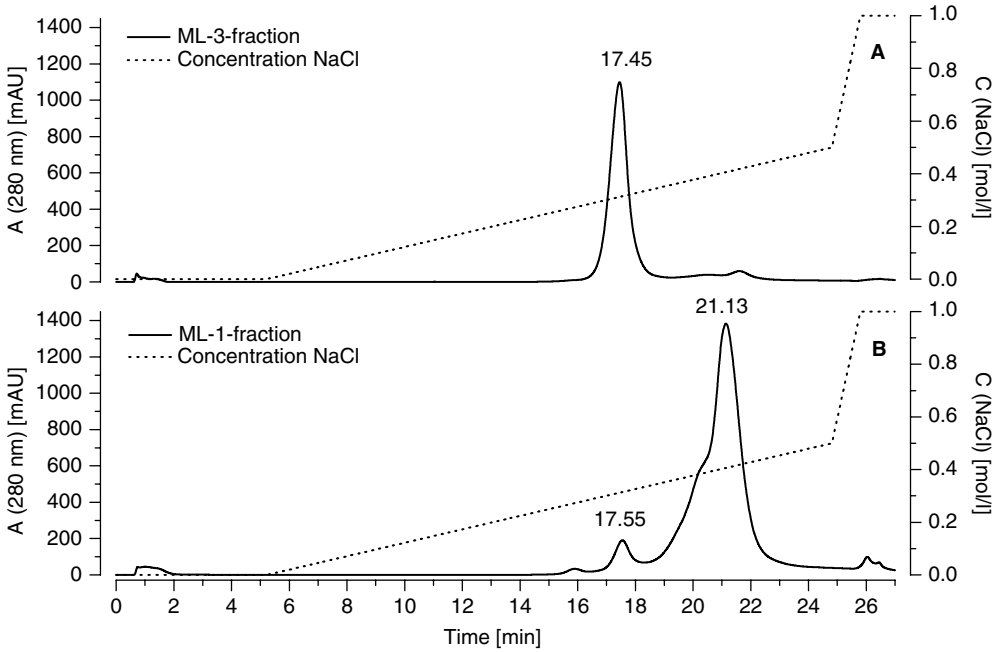

Figure 2 Purification of ML-3 (A) and ML-1 (B) by cation exchange rechromatography on a MonoS HR5/5 column (5 × 50 mm) with a linear sodium chloride gradient from 0 to 0.6 M in 9.82 min; buffer A: 15 mM sodium citrate, pH 4.2; buffer B: 1 M sodium chloride in buffer A; flow rate: 1.0 ml/min; detection wavelength: 280 nm.

detectable with molecular weights of 32 000 (ML-3B), 28 000 (ML-3A), 35 000 (ML-1B) and 29 000 (ML-1A), indicating that both chains of ML-3 have smaller molecular weights than the corresponding A and B chains of ML-1, respectively. Though no reducing agent was added to the sample (Figure 3B), both chains were detectable to a lesser extent also for ML-1 (Figure 3A). Separated chains were observed in SDS-PAGE electropherograms frequently so far only for ML-1, but not for ML-3. For further analysis, laser desorption mass spectra of the lectins were recorded with a TOF-MALDI-MS in linear mode using the sandwich sample preparation method and *trans*-ferulic acid as matrix (Figure 4). The mass spectra revealed a m/z value of about 59 300 for ML-3, in contrast to 61 900 for ML-1, confirming the results received from SDS-PAGE.

Primary Structure Determination of ML-3B

The purified protein was reduced with β-mercaptoethanol, and then the cysteine residues were vinylpyridinylated. The mixture of the alkylated A and B chains were desalted by dialysis and treated with trypsin and chymotrypsin, respectively. After separating the cleaved peptide fragments by RP-HPLC (Figure 5), all purified fractions were analysed by automated Edman sequencing and the complete primary structure of ML-3B could be established by alignment of overlapping peptide fragments of the tryptic and chymotryptic digest, respectively. The results of the sequencing data are collected in Figure 6. For all selected peptide fragments the sequences could be determined unequivocally as further verified by MALDI-MS (Table 1).

ML-3B is constituted of 262 amino acid residues, including ten cysteine residues. The molecular weight of the protein chain is calculated to be 28 362.8 Da not including the carbohydrate side chains, coinciding with the results gained from SDS-PAGE (Figure 3). For the amino acid residues corresponding to positions 51, 123 and 262 three residue substitutions were detected as shown in Table 2.

The amino acid composition, calculated from the sequencing results, is in good agreement with the values for the extrapolated number of amino acid residues based on amino acid analysis determination of purified ML-3 (Table 3) within the methodical range of variation.

Carbohydrate Composition Analysis

The monosaccharide composition analysis of ML-3, achieved via hydrolysis of protein samples and HPLC quantification of released PMP derivatives of reducing monosaccharides, revealed the occurrence of high mannose type glycans and traces of xylose (Table 4, Figure 7). Contrary to ML-3, for ML-1 a

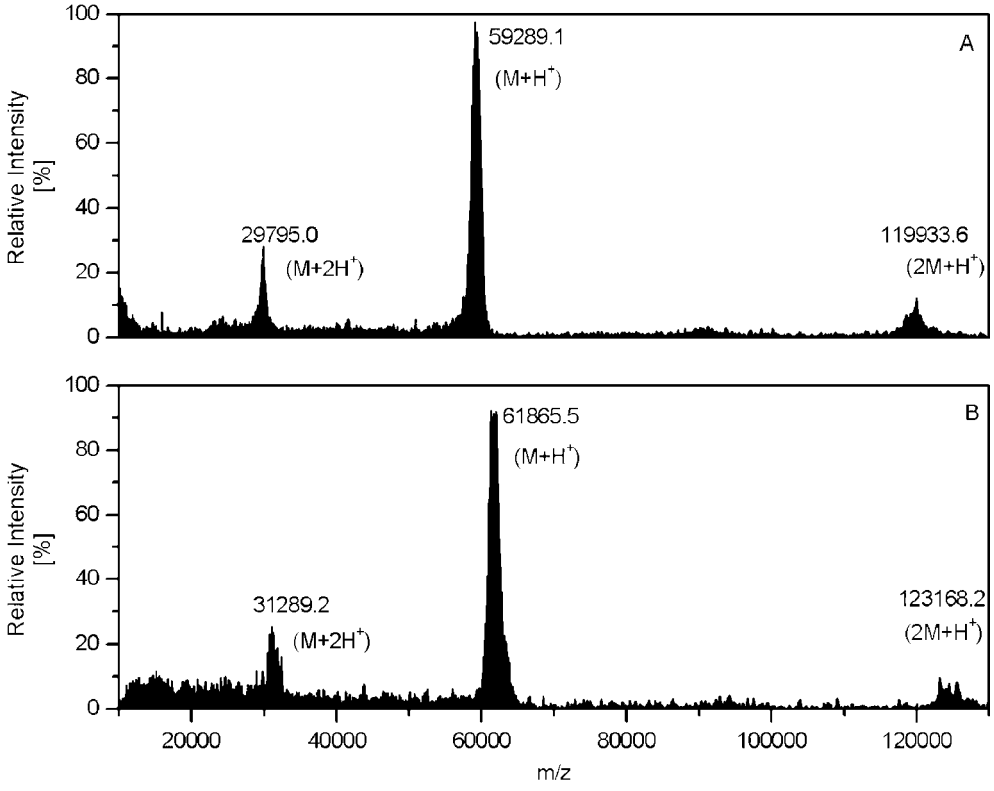

Figure 4 MALDI-MS spectra of ML-3 (A) and ML-1 (B). Matrix: *trans*-ferrulic acid, number of shots : 50, laser power: 94, wavelength: 337 nm.

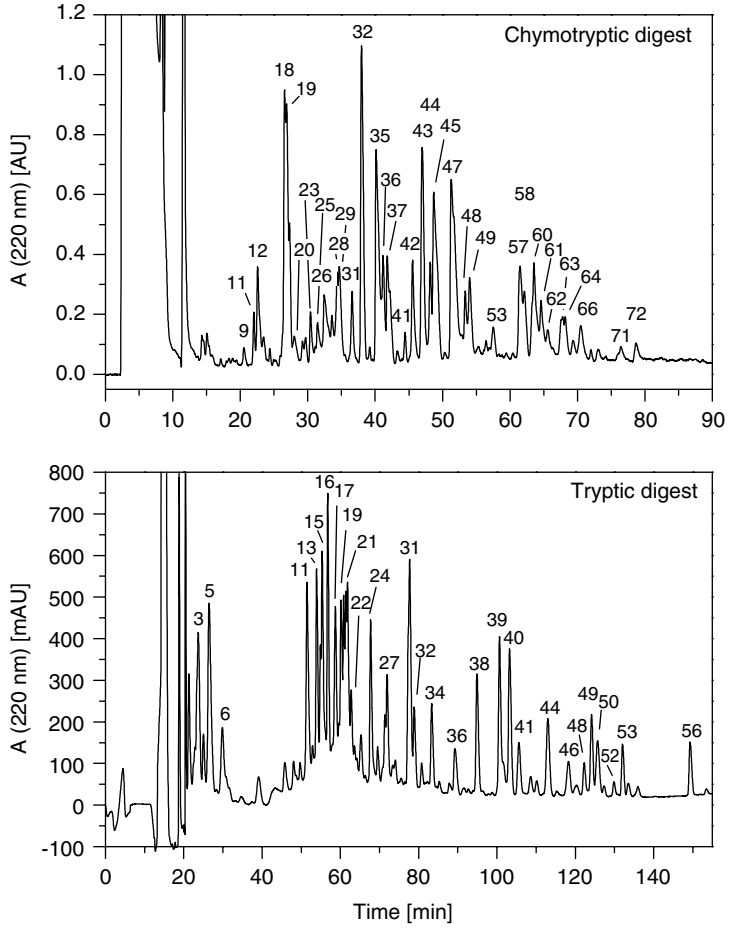

Figure 5 RP-HPLC chromatograms of the chymotryptic (top) and tryptic (bottom) digests of ML-3, respectively. Peptide fractions were collected manually and labeled according to the figure. Chromatographic conditions: Columns: Gromsil C-18 column (100-5 ODS, 4.6 × 250 mm, for chymotryptic digest), Nucleosil 100-7 RP 18 column (10 × 250 mm, for tryptic digest); buffer A: 0.1% (v/v) TFA/water; buffer B: 80% (v/v) CH_3CN, 20% (v/v) water, 0.1% (v/v) TFA; gradient elution for chymotryptic digest: 10% B (0–5 min), 10%–60% B (5–105 min), 60%–100% B (105–115 min); gradient elution for tryptic digest: 10% B (0–13 min), 10%–30% B (13–33 min), 30%–60% B (33–90 min), 60%–100% B (90–108 min), 100% B (108–160 min); flow rate: 1.0 ml/min; detection wavelength: 220 nm.

significantly lower ratio of mannose to GlcNAc was found besides the presence of fucose, indicating a different glycosylation profile for the N-glycosylation sites of ML-1 (4 sites) compared with those of ML-3 (2 sites). It proved to be difficult to separate traces of contaminating carbohydrates from ML-1 and ML-3, used for elution from the affinity column, without losing activity. Therefore, occasionally observed varying amounts of galactose and glucose were not considered to be structural components of either mistletoe lectin. Despite the restrictions of this method concerning quantification, especially for the more hydrophobic PMP derivatives of xylose and fucose, the following averaged monosaccharide composition for ML-3 can be assumed: $GlcNAc_2 : Man_5 : Xyl_{0.5}$.

Glycan Structure Analysis

Two N-type glycosylation sites were identified by sequence analysis at position N^{B95} (NGT) and N^{B135} (NDT). The site-specific glycosylation profile of ML-3B was analysed by treatment of aliquots of the tryptic glycopeptides T7 (E^{B86}-R^{B102}) and T8 (S^{B103}-R^{B140}) with peptide-N-glycosidase F, α1-2,3,6-mannosidase (Jack bean), α1-2,3-mannosidase (*rec. E. coli*) and α1-2-mannosidase (*Aspergillus satoi*) for 24 h (Figure 8, Table 5). 1 µl aliquots of the samples were examined by MALDI-MS after 2 and 24 h. From the mass decreases observed in the mass spectra of the treated glycopeptides the number of carbohydrates could be determined, while the linkages of the carbohydrate chains followed from the glycosidase specificity. For each glycosylation site different high mannose type glycoforms were identified and the structures (I) — (IV) shown in Figure 8 are suggested. To the N-glycosylation site at position N^{B95} (NGT) a hexamannosyl octasaccharide (I, HPLC fraction C43, Figure 5) and to a lesser extent a pentamannosyl heptasaccharide (II, present in the HPLC fraction C44,

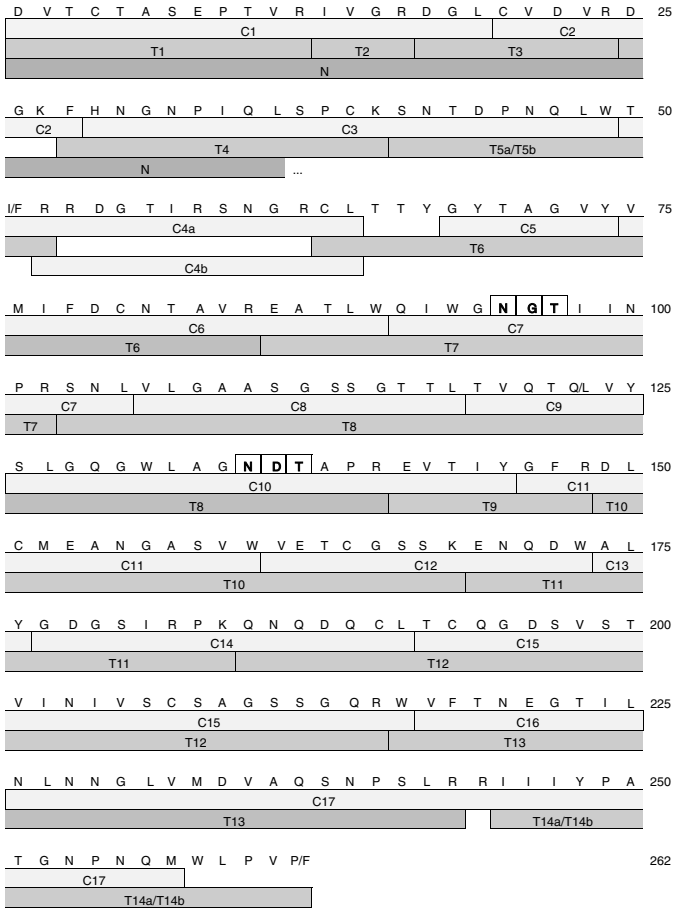

Figure 6 Amino acid sequence and sequencing strategy of the ML-3B chain. C and T indicate peptides from chymotrypsin and trypsin digests, respectively. N represents the aminoterminal sequence determined from native protein, the amino acid residues of N-glycosylation sites are boxed bold.

Figure 5, at the amount ratio (C44/C43) of about 0.2 based on HPLC peak area) are attached. Two different glycoforms with identical amino acid sequence (peptide T8, Table 1) are linked to the glycosylation site N^{B135} (NDT): xylomannosyl type oligosaccharides with 6 (IV) or 7 (III) carbohydrate residues. The monosaccharide composition of ML-3 calculated from these results (GalNAc 2 : Man 5: Xyl 0.5) is the same as that obtained from the monosaccharide composition analysis.

Sequence Comparison and Homology Model of ML-3

As expected, the online comparison of the amino acid sequence of ML-3B with other known protein sequences revealed a high degree of sequence conservation compared with ML-1B and with other B chains of type-II RIPs.

Subsequently, the sequence alignment (Figure 9) with the highest rated PDB-database entries 1CE7 (ML-1 from *Viscum album L. album*), 2AAI (ricin from *Ricinus communis*) and 1ABR (abrin from *Abrus precatorius*) yielded overall identity values of 77%, 65% and 54%, respectively. With the BLOSUM 62 similarity matrix, the percentage of conserved amino acid residues is increasing to 83%, 78% and 70%, respectively.

For further structural characterization, a preliminary homology model of ML-3 was prepared with the *SWISS-Model* online model server in the first approach mode [31–33] using the x-ray diffraction-derived templates 1CE7 (ML-1), 1ABR (abrin a), 2AAI (ricin) and the recently published ML-3 A chain [1]. The superposition of the protein backbone of ML-3 with ML-1, ricin and abrin demonstrates a similar overall fold (Figures 10 and 11).

While the ML-3A-chain is composed of α-helices and β-sheets, the ML-3B-chain shows an all-beta conformation and consists of two globular domains 1 and 2. Each of the domains is initiated by a linker domain $\lambda 1$ and $\lambda 2$, followed by three homologous carbohydrate-binding subdomains $\alpha 1$, $\beta 1$, $\gamma 1$ and $\alpha 2$, $\beta 2$, $\gamma 2$, respectively (Figure 11). The model enabled us to assign unconstrained disulphide bridges to the cysteine residues (Figure 12). The cysteine residue detected at position Cys^{B4} of ML-3 is linked via a disulphide bridge to the cysteine residue Cys^{A247} located at the *C*-terminus of the A chain. Four disulphide bridges stabilize the

Table 1 Results of the Sequence Analysis of Peptides, Isolated from the Chymotryptic (C) and Tryptic (T) Digest of ML-3B. HPLC Fractions and Identified Peptides are Labeled According to Figures 5 and 6

Fraction (HPLC)	Peptide	Position	Sequence	Mth[a] [Da]	Mob[b] [Da]
11	T1	1–12	DVTCTASEPTVR	1383.5	1385.1
5	T2	13–16	IVGR	443.5	444.3
19	T3	17–24	DGLCVDVR	981.1	982.0
21	T4	28–40	FHNGNPIQLSPCK	1559.8	1564.1
34	T5a	41–52	SNTDPNQLWTFR	1478.6	1480.2
31	T5b	41–52	SNTDPNQLWTIR	1444.5	1445.1
13	T6	63–85	CLTTYGYTAGVYVMIFDCNTAVR	2772.3	2772.9
39	T7	86–102	EATLWQIWG**NGT**IINPR	1969.2	3350.4
16	T8	103–140	SNLVLGAASGSSGTTLTVQTLVYSLGQGWLAG**NDT**APR	3764.2	4952.5 4791.4
32	T9	141–148	EVTIYGFR	984.1	985.5
27	T10	149–168	DLCMEANGASVWVETCGSSK	2297.6	2299.7
24	T11	169–184	ENQDWALYGDGSIRPK	1847.9	1848.7
7	T12	185–215	QNQDQCLTCQGDSVSTVINIVSCSAGSSGQR	3501.8	3503.8
15	T13	216–243	WVFTNEGTILNLNNGLVMDVAQSNPSLR	3103.5	3104.4
44	T14a	245–262	IIIYPATGNPNQMWLPVF	2074.5	2076.2
46	T14b	245–262	IIIYPATGNPNQMWLPVP	2024.4	2045.2
42	C1	1–20	DVTCTASEPTVRIVGRDGL	2094.4	2095.1
26	C2	21–28	CVDVRDGKF	1143.3	1144.2
47	C3	29–49	HNGNPIQLSPCKSNTDPNQLW	2468.7	2470.8
26	C4a	50–64	TIRRDGTIRSNGRCL	1823.1	1824.2
20	C4b	52–64	RRDGTIRSNGRCL	1608.8	1608.5
19	C5	68–74	GYTAGVY	729.8	730.7
63	C6	75–90	VMIFDCNTAVREATLW	1974.3	1976.2
44	C7	91–105	QIWG**NGT**IINPRSNL	1682.9	2901.8
23	C8	106–118	VLGAASGSSGTTL	1120.2	1122.5
11	C9	119–125	TVQTQVY	837.9	839.9
49	C10	126–145	SLGQGWLAG**NDT**APREVTIY	2148.4	3174.9
53	C11	146–160	GFRDLCMEANGASVW	1761.0	1764.5
18	C12	161–173	VETCGSSKENQDW	1587.7	1589.9
12	C13	174–176	ALY	365.4	—
18	C14	177–191	GDGSIRPKQNQDQCL	1763.9	1764.8
60	C15	192–217	TCQGDSVSTVINIVSCSAGSSGQRW	2753.1	2756.6
42	C16	218–225	VFTNEGTIL	993.1	994.4
63	C17	226–257	NLNNGLVMDVAQSNPSLRRIIIYPATGNPNQM	3512.0	3512.9

[a] Calculated mass (M).
[b] Observed mass ($M + H^+$).

Table 2 Identified Amino Acid Variants of ML-3B

Position	Amino acid residue	Variant
51	I	F
123	Q	L
262	P	F

subdomains $\alpha 1$ (Cys^{B20}-Cys^{B39}), $\beta 1$ (Cys^{B63}-Cys^{B80}), $\alpha 2$ (Cys^{B151}-Cys^{B164}) and $\beta 2$ (Cys^{B190}-Cys^{B207}). According to this model, a further cysteine residue at position Cys^{B193} remains unbound.

DISCUSSION

From extracts of the European mistletoe, three isolectins can be isolated [16–18]. These isoforms have different monosaccharide specificities and molecular masses. ML-1 specifically binds to D-galactose, ML-3 to *N*-acetyl-D-galactosamine and for ML-2 binding sites for both carbohydrates with similar binding constants were detected [16–18]. Recently, the complete primary structure of the ML-3A chain was reported [1]. The complete primary structure was determined using proteolytic digests of ML-3A, HPLC separation of the peptides, Edman degradation and MALDI-MS. ML-3A consists of 254 amino acid residues, showing a high homology to the A chain of isolectin ML-1 with

Table 3 Amino Acid Analysis of ML-3

AA	Conc. (AA) [nmol/ml]	Number (AA) experimental	Number (AA) theoretical[b]	Weight proportion (AA) [%]	Theoretical[b] weight proportion (AA) [%]
Asx[a]	251.1	60.4	58	11.7	11.2
Thr	184.4	44.3	42	8.6	8.1
Ser	194.6	46.8	48	9.1	9.3
Glx[a]	189.0	45.4	49	8.8	9.5
Pro	93.8	22.5	22	4.4	4.3
Gly	177.8	42.7	44	8.3	8.5
Ala	129.1	31.0	31	6.0	6.0
Cys	46.4	11.2	11	2.2	2.1
Val	156.4	37.6	37	7.3	7.2
Met	29.2	7.0	8	1.4	1.6
Ile	140.6	33.8	33	6.6	6.4
Leu	181.2	43.6	44	8.4	8.5
Tyr	63.1	15.2	17	2.9	3.3
Phe	70.4	16.9	18	3.3	3.5
His	14.8	3.6	4	0.7	0.8
Lys	29.6	7.1	4	1.4	0.8
Arg	153.6	36.9	36	7.2	7.0
Trp	—	[b]10.0	10	1.9	1.9
Sum		516	516		

[a] Asn and Gln are detected as Asp and Glu, respectively.
[b] Calculated from sequencing data.

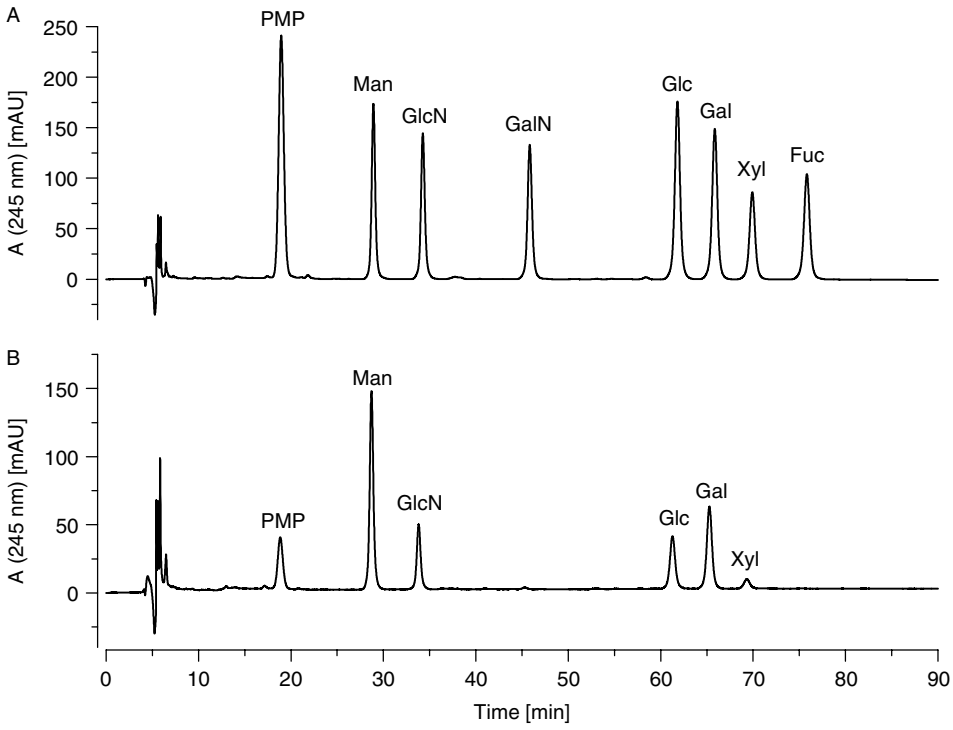

Figure 7 HPLC chromatograms of the monosaccharide composition analysis. (A) PMP derivatives of the monosaccharide standard mixture containing 5 nmol of mannose (Man), *N*-acetylgalactosamine (GalNAc), *N*-acetylglucosamine (GlcNAc), galactose (Gal), glucose (Glc), xylose (Xyl) and fucose (Fuc), respectively. (B) PMP derivatives of monosaccharides released by hydrolysis of 80 μg ML-3. During hydrolysis, GalNAc and GlcNAc are deacetylated to galactosamine (GalN) and glucosamine (GlcN), respectively. Chromatographic conditions: Column: Hypersil HyPurity Elite C18-5 (4.6 × 250 mm, ThermoQuest, Runcorn, UK); buffer A: 0.1 M ammonium acetate, 10% (v/v) CH_3CN, pH 5.5; buffer B: 0.1 M ammonium acetate, 25% (v/v) CH_3CN, pH 5.5; gradient elution: 45% B (0–5 min), 45%–100% B (5–50 min), 100% B (50–90 min); flow rate: 1 ml/min; detection wavelength: 245 nm.

Table 4 Monosaccharide Composition Analysis of ML3 and ML1

Mono-saccharide	ML-3			ML-1		
	Amount [nmol]	Normalized[b] amount [nmol]	Content [%$_{mol}$]	Amount [nmol]	Normalized[b] amount [nmol]	Content [%$_{mol}$]
Man	5.19	4.99	67.0	5.97	3.91	60.1
GlcN	2.10	2.00	26.8	3.13	2.00	30.7
GalN	—	—	—	—	—	—
Glc	—[a]	—	—	—[a]	—	—
Gal	—[a]	—	—	—[a]	—	—
Xyl	0.48	0.46	6.2	0.80	0.52	8.0
Fuc	—	—	—	0.11	0.08	1.2
Sum	7.77	7.45	100.0	10.01	6.51	100.0

[a] Variable traces, originating from lactose or galactose bound to lectin during its isolation.
[b] Normalized values related to a GlcN amount of 2.00 nmol.

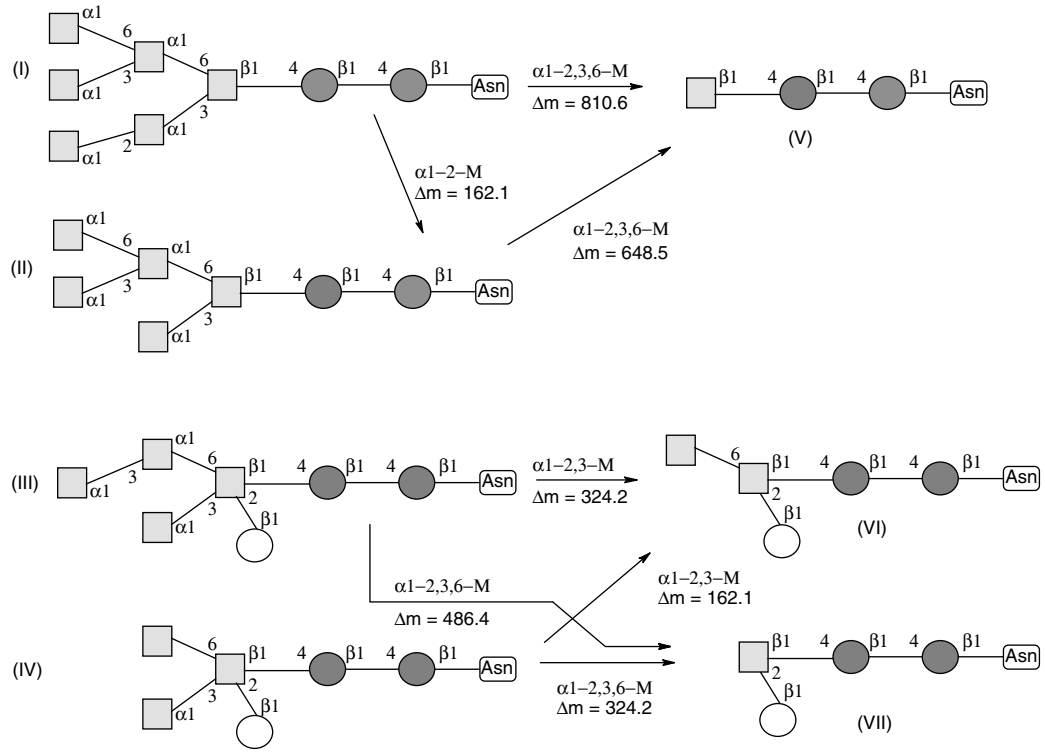

Figure 8 Schematic representation of identified glycan structures of ML-3B by gradual degradation of the glycopeptides T7 (E^{86}-R^{102}) and T8 (S^{103}–R^{140}) with specific mannosidases (M). Mannose residues are represented as grey squares, N-acetylglucosamine residues as dark circles and xylose residues by light circles. Structures (I) and (II) were identified as glycoforms of the first glycosylation site (N^{95}), whereas structures (III) and (IV) could be assigned to the second glycosylation site (N^{135}).

exchanges of 24 amino acid residues. An important structural difference compared with ML-1A is the lack of the single N-glycosylation site in ML-3A due to an amino acid exchange at position 112 (ML-1A: $N^{112}GS \Rightarrow$ ML-3A: $T^{112}GS$). Sequence comparison of ML-3A with the A chains of other RIPs of type II verified the rigid conservation of all amino acid residues, responsible for the RNA-N-glycosidase activity as reported for ricin D [9,40,41].

The structure determination of ML-3B presented in this report reveals a homologous sequence compared with the B chains of mistletoe lectin-1, ricin and abrin. Similar to the B chains of ricin and ML-1, the sequence of ML-3B is composed of six homologous carbohydrate-interacting subdomains (Figures 11–12), most likely as a result of a series of evolutionary gene duplications of an ancestral carbohydrate-binding peptide [24]. All up to date sequenced type-II RIP B-chains share an

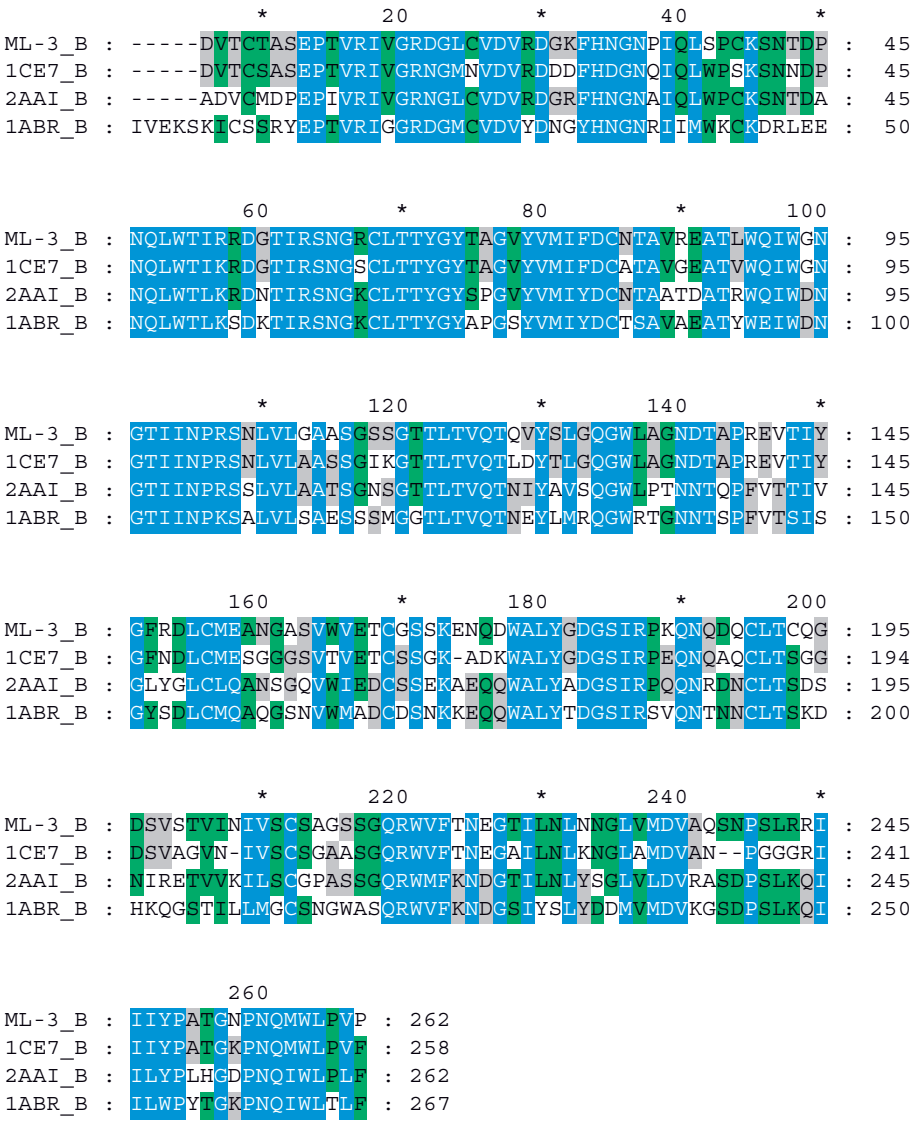

Figure 9 Multiple sequence alignment of the B chains of ML-3 (ML-3_B), ML-1 (PDB: 1CE7_B), ricin (PDB: 2AAI_B) from *Ricinus communis* and abrin (PDB: 1ABR_B) from *Abrus precatorius*. Similar amino acid residues are shaded using a Blosum 62 scoring table (blue 100%, green 75%, grey 50%).

analogous pattern. For ricin, two of the carbohydrate-binding subdomains, 1α and 2γ, remained active, while the others lack activity due to sterical hindrance or amino acid residue exchanges of some key residues [24,25,34]. The carbohydrate-binding ability of the subdomains seems to be due to five key residues: for the so-called 'low affinity site' with galactosyl-specificity, located at the 1α subdomain, the residues Asp^{B22}, Trp^{B37}, Gln^{B35}, Asn^{B46} and Gln^{B47} were identified. For the 'high affinity site', with additional binding affinity to GalNAc [34], the residues Asp^{B234}, Tyr^{B248}, Ile^{B246}, Asn^{B255} and Gln^{B256} were determined to be responsible for lectin activity. Based on these structural considerations, a Gal and GalNAc specificity is observed for ricin. On top of both carbohydrate-binding pockets, the aromatic side chains of Trp^{B37} and Tyr^{B248} are located and the exchange of these aromatic residues against His ([34] in RCA) or Ser ([35] in SNAI') in other type-II RIP B chains leads to a decrease in monosaccharide affinity or an altered monosaccharide specificity. For ML-3B, an exchange was found of this important aromatic side chain of the low affinity site against a serine residue (ricin: Trp^{B37} $\rightarrow$ ML-3: Ser^{B37}), probably resulting in a decreased galactose affinity. In contrast to ML-1B, the high affinity site of ML-3B is nearly identical to that found for ricin [34] showing affinity for Gal and GalNAc. It is assumed that due to this structural similarity of the high affinity carbohydrate binding site of the ricin B and ML-3

Table 5 Mass Spectroscopic Determination of Specific Glycosidase Cleavages from Glycopeptides of ML-3B

Glycopeptide	Glycosidase	Incubation time [h]	*m/z* after glycosidase treatment		Remaining glycan composition
^{86}EATLWQIWG**NGT**IINPR^{102}	PNGase-F (rec. *E. coli*)	24	1993.2 $(M+Na)^+$		—
MW 1969.2					
m/z 3350.4 $(M+H)^+$					
$\Delta m = 1381.2 \equiv N_2H_6$ (1379.0 Da) (I)	α1-2,3,6-Mannosidase (Jack bean)	2	2862.0		N_2M_3
			2704.8		N_2M_2
		24	2539.0	(V)	N_2M_1
	α1-2-Mannosidase (*Aspergillus satoi*)	24	3188.5	(II)	N_2M_5
^{103}SNLVLGAASGSSGTTLTVQTLVYSL GQGWLAG**NDT**APR^{140}	PNGase-F (rec. *E. coli*)	24	3766.8		—
MW 3764.2					
m/z 4952.5 and 4791.4 $(M+H)^+$	α1-2,3-Mannosidase (rec. *E. coli*)	24	4792.2		$N_2M_3X_1$
$\Delta m = 1188.3 \equiv N_2H_4X_1$ (1186.9 Da) (III)			4630.3	(VI)	$N_2M_2X_1$
$\Delta m = 1027.2 \equiv N_2H_3X_1$ (1024.8 Da) (IV)	α1-2,3,6-Mannosidase (Jack bean)	2	4631.2		$N_2M_2X_1$
			4465.9	(VII)	$N_2M_1X_1$
		24	4465.9	(VII)	$N_2M_1X_1$

N, N-acetylglucosamine; M, Mannose; X, Xylose; identified glycan structures are given in Roman numbers in parentheses (see Figure 8).

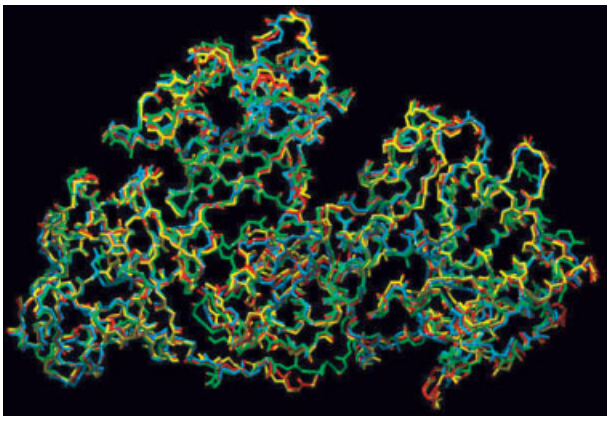

Figure 10 Peptide backbone overlay of ML-3 (red, model), ML1 (blue, PDB: 1CE7), ricin (yellow, PDB: 2AAI) and abrin (green, PDB: 1ABR).

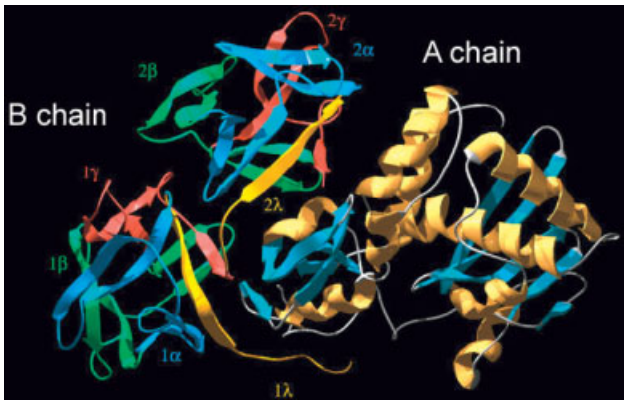

Figure 11 Cartoon plot of the ML3 homology model. α-Helices of the A chain are drawn in orange and β-sheet structures in blue. Subdomains of the B chain are coloured in orange (λ), blue (α), green (β) and red (γ), respectively. The homology model of ML3 was prepared by the SWISS-Model server in the first approach mode using x-ray diffraction-derived templates from the pdb database 1CE7 (ML-1), 1ABR (abrin a), 2AAI (ricin).

B chain the latter is enabled to bind specifically *N*-acetylgalactosamine and lactose.

The glycan analysis of ML-3B reveals different glycans of the N-type. The first two, linked to Asn^{B95}, are triantennary hexamannosyl octasaccharides (I) and pentamannosyl heptasaccharides (II), respectively, of high mannose type which could be identified at the same binding site of other type-II RIP B chains (ricin d, RCA, abrin, ML1B) [36–39]. Two different carbohydrate chains were found to be attached to

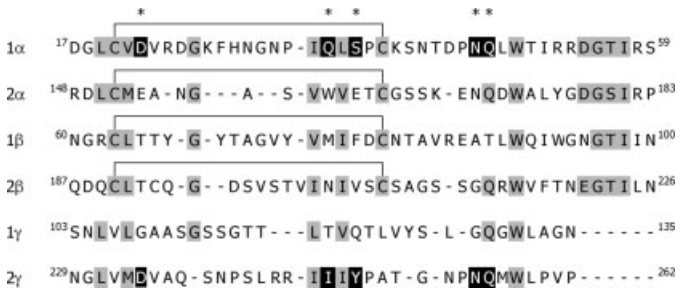

Figure 12 Alignment of the six homologous subdomains of ML-3B. Conserved amino acid residues are shaded in grey, disulphide-bridges are indicated by connection lines, the positions of key residues of carbohydrate binding sites are marked with asterisks and the corresponding residues of the active 1α and 2γ subdomains are shaded in black.

Asn^{B135}, a trimannosyl xylosyl hexasaccharide (IV) and a tetramannosyl xylosyl heptasaccharide (III), oligosaccharides also identified for other type-II RIP B chains, such as those of ricin, RCA and abrin [36–38].

Three main differences concerning the glycosylation profile of ML-3 compared with ML-1 should be pointed out: firstly, compared with ML-1A, the A-chain of ML-3 is not glycosylated [1]. Secondly, the third N-glycosylation site, present in the B chain of ML-1 (Asn^{B61}-Gly-Ser^{B63}) is lost due to a mutation of a serine to an arginine residue (Asn^{B60}-Gly-Arg^{B62}). Thirdly, the oligosaccharide chains bound to the N-glycosylation site at position Asn^{B135}-Asp-Thr^{B137} of ML-3B (III, IV) are different compared with those of ML-1B (I, II) at position Asn^{B136}-Asp-Thr^{B138}.

Despite the close similarity of the overall structure of ML-3 and ML-1, remarkable differences in the physiological activities were observed. The cytotoxicity of ML-3 against cultured human leukaemia Molt 4 cells and human monocytes was reported to be about 10 times higher compared with ML-1 [42]. The stimulation of cytokine release (IL-1α, IL-1β and TNF-α) of cultured monocytes, treated with nontoxic doses of mistletoe lectins, was found to be different for ML1, ML-2 and ML-3 [7]. Furthermore, the effectiveness of ML-3 to induce apoptosis in cultured human lymphocytes was described to be higher compared with ML-1 [43]. As the primary and three-dimensional structures between ML-3 and ML-1 are very close, it is assumed that the pronounced differences in their biological activities are mainly based on their different glycosylation patterns and different carbohydrate binding sites of both glycoproteins.

The protein sequences reported in this paper have been submitted to the Swiss-Prot database under the accession codes P87800 (ML-3B) and P82683 (ML-3A).

REFERENCES

1. Wacker R, Stoeva S, Pfüller K, Pfüller U, Voelter W. Complete structure determination of the A chain of Mistletoe lectin III from *Viscum album* L. ssp *album*. *J. Pept. Res.* 2004; **10**: 138–148.
2. Baxevanis CN, Voutsas IF, Soler MH, Gritzapis AD, Tsitsilonis OE, Stoeva S, Voelter W, Arsenis P, Papamichail M. Mistletoe lectin I-induced effects on human cytotoxic lymphocytes. I. Synergism with IL-2 in the induction of enhanced LAK cytotoxicity. *Immunopharmacol. Immunotoxicol.* 1998; **20**: 355–372.
3. Beuth J, Stoffel B, Ko HL, Jeljaszewicz J, Pulverer G. Immunomodulating ability of galactoside-specific lectin standardized and depleted mistletoe extract. *Arzneimittelforsch/Drug Res.* 1995; **45**: 1240–1242.
4. Hajto T, Hostanska K, Gabius HJ. Modulatory potency of the beta-galactoside-specific lectin from mistletoe extract (Iscador) on the host defense system *in vivo* in rabbits and patients. *Cancer Res.* 1989; **49**: 4803–4808.
5. Hajto T, Hostanska K, Frei K, Rordorf C, Gabius HJ. Increased secretion of tumor necrosis factors alpha, interleukin 1, and interleukin 6 by human mononuclear cells exposed to beta-galactoside-specific lectin from clinically applied mistletoe extract. *Cancer Res.* 1990; **50**: 3322–3326.
6. Möckel B, Schwarz T, Zinke H, Eck J, Langer M, Lentzen H. Effects of mistletoe lectin I on human blood cell lines and peripheral blood cells. Cytotoxicity, apoptosis and induction of cytokines. *Arzneimittelforsch/Drug Res.* 1997; **47**: 1145–1151.
7. Ribereau-Gayon G, Dumont S, Muller C, Jung ML, Poindron P, Anton R. Mistletoe lectins I, II and III induce the production of cytokines by cultured human monocytes. *Cancer Lett.* 1996; **109**: 33–38.
8. Beuth J, Ko HL, Tunggal L, Buss G, Jeljaszewicz J, Steuer MK, Pulverer G. Immunaktive Wirkung von Mistellektin-1 in Abhängigkeit von der Dosierung. *Arzneimittelforsch/Drug Res.* 1994; **44**: 1255–1258.
9. Barbieri L, Battelli MG, Stirpe F. Ribosome-inactivating proteins from plants. *Biochim. Biophys. Acta* 1993; **1154**: 237–282.
10. Endo Y, Mitsui K, Motizuki M, Tsurugi K. The mechanism of action of ricin and related toxic lectins on eukaryotic ribosomes. *J. Biol. Chem.* 1987; **262**: 5908–5912.
11. Frantz M, Jung ML, Ribereau-Gayon G, Anton R. Modulation of mistletoe lectins cytotoxicity by carbohydrates and serum glycoproteins. *Arzneimittelforsch/Drug Res.* 2000; **50**: 471–478.
12. Doser C, Doser M, Hülsen H, Mechelke F. Influence of carbohydrates on the cytotoxicity of an aqueous mistletoe drug and of purified mistletoe lectins tested on human T-leukemia cells. *Arzneimittelforsch/Drug Res.* 1989; **39**: 647–651.
13. Alovskaya AA, Safronova VG, Kornilov VV, Kornev AN, Savochkina YM, Krauspenhaar R, Betzel C, Voelter W, Mikhailov AM. Viscumin modulates the neutrophil respiratory burst induced by a chemotactic peptide. *Biophysics* 2000; **45**: 669–675.
14. Bantel H, Engels IH, Voelter W, Schulze-Osthoff K, Wesselborg S. Mistletoe lectin activates caspase-8/FLICE independently of death receptor signaling and enhances anticancer drug-induced apoptosis. *Cancer Res.* 1999; **59**: 2083–2090.
15. Vervecken W, Kleff S, Pfüller U, Büssing A. Induction of apoptosis by mistletoe lectin I and its subunits. No evidence for cytotoxic

effects caused by isolated A- and B-chains. *Int. J. Biochem. Cell. Biol.* 2000; **32**: 317–326.
16. Franz H, Ziska P, Kindt A. Isolation and properties of three lectins from mistletoe (*Viscum album* L.). *Biochem. J.* 1981; **195**: 481–484.
17. Samtleben R, Kiefer M, Luther P. Characterization of the different lectins from *Viscum album* (Mistletoe) and their structural relationships with the agglutinins from *Abrus precatorius* and *Ricinus communis*. *Lectins: Biol. Biochem. Clin. Biochem.* 1985; **4**: 617–626.
18. Eifler R, Pfüller K, Göckeritz W, Pfüller U. Improved procedures for isolation of mistletoe lectins and their subunits: lectin pattern of the european mistletoe. *Lectins: Biol. Biochem. Clin. Biochem.* 1993; **9**: 144–151.
19. Soler MH, Stoeva S, Schwarmborn C, Wilhelm S, Stiefel T, Voelter W. Complete amino acid sequence of the A chain of mistletoe lectin I. *FEBS Let.* 1996; **399**: 153–157.
20. Soler MH, Stoeva S, Voelter W. Complete amino acid sequence of the B chain of mistletoe lectin I. *Biochem. Biophys. Res. Commun.* 1998; **246**: 596–601.
21. Eck J, Langer M, Möckel B, Rothe M, Zinke H, Lentzen H. Cloning of the mistletoe lectin gene and characterization of the recombinant A-chain. *Eur. J. Biochem.* 1999; **264**: 775–784.
22. Eck J, Langer M, Möckel B, Witthohn K, Zinke H, Lentzen H. Characterization of recombinant and plant-derived mistletoe lectin and their B-chains. *Eur. J. Biochem.* 1999; **265**: 788–797.
23. Krauspenhaar R, Eschenburg S, Perbandt M, Kornilov V, Konareva N, Mikailova I, Stoeva S, Wacker R, Maier T, Singh T, Mikhailov M, Voelter W, Betzel C. Crystal structure of mistletoe lectin I from *Viscum album*. *Biochem. Biophys. Res. Commun.* 1999; **257**: 418–424.
24. Villafranca JE, Robertus JD. Ricin B chain is a product of gene duplication. *J. Biol. Chem.* 1981; **256**: 554–556.
25. Rutenber E, Ready M, Robertus JD. Structure and evolution of ricin B chain. *Nature* 1987; **326**: 624–626.
26. Laemmli UK. Cleavage of structural proteins during the assembly of the head of bacteriophage T4. *Nature* 1970; **227**: 680–685.
27. Friedman M, Krull LH, Cavins JF. The chromatographic determination of cystine and cysteine residues in proteins as S-β-(4-pyridylethyl)cysteine. *J. Biol. Chem.* 1970; **245**: 3868–3871.
28. Shevchenko A, Wilm M, Vorm O, Mann M. Mass spectrometric sequencing of proteins from silver-stained polyacrylamide gels. *Anal. Chem.* 1996; **68**: 850–858.
29. Honda S, Akao E, Suzuki S, Okuda M, Kakehi K, Nakamura J. High performance liquid chromatography of reducing carbohydrates as strongly ultraviolet-absorbing and electrochemically sensitive 1-phenyl-3-methyl-5-pyrazolone derivatives. *Anal. Biochem.* 1989; **180**: 351–357.
30. Fu D, O'Neill RA. Monosaccharide composition analysis of oligosaccharides and glycoproteins by high-performance liquid chromatography. *Anal. Biochem.* 1995; **227**: 377–384.
31. Guex N, Peitsch MC. SWISS-MODEL and the Swiss-PdbViewer: An environment for comparative protein modelling. *Electrophoresis* 1997; **18**: 2714–2723.
32. Peitsch MC. ProMod and Swiss-Model: Internet-based tools for automated comparative protein modelling. *Biochem. Soc. Trans.* 1996; **24**: 274–279.
33. Peitsch MC. Protein modeling by e-mail. *Bio/Technology* 1995; **13**: 658–660.
34. Rutenber E, Robertus JD. Structure of ricin B-chain at 2.5 Å resolution. *Proteins* 1991; **10**: 260–269.
35. Van Damme EJM, Roy S, Barre A, Citores L, Mostafapous K, Rouge P, van Leuven F, Girbes T, Goldstein IJ, Peumans PJ. Elderberry (*Sambucus nigra*) bark contains two structurally different Neu5Ac(α2,6)Gal/GalNAc-binding type 2 ribosome-inactivating proteins. *Eur. J. Biochem.* 1997; **245**: 648–655.
36. Kimura Y, Hase S, Kobayashi Y, Kyogoku Y, Ikenaka T, Funatsu G. Structures of sugar chains of ricin D. *J. Biochem.* 1988; **103**: 944–949.
37. Kimura Y, Hase S, Kobayashi Y, Kyogoku Y, Ikenaka T, Funatsu G. Structures of sugar chains of *Ricinus communis* agglutinin. *Biochim. Biophys. Acta* 1988; **966**: 248–256.
38. Kimura Y, Hase S, Ikenaka T, Funatsu G. Structures of sugar chains of abrin a obtained from *Abrus precatorius* seeds. *Biochim. Biophys. Acta* 1988; **966**: 150–159.
39. Stoeva S, Maier T, Soler MH, Voelter W. Carbohydrate chains and their binding sites in Mistletoe lectin I. *Polish J. Chem.* 1999; **73**: 125–133.
40. Chen X, Link TM, Schramm VL. Ricin A-chain: Kinetics, mechanism, and RNA stem-loop inhibitors. *Biochemistry* 1998; **37**: 11 605–11 613.
41. Yan X, Day P, Hollis T, Monzingo AF, Schelp E, Robertus JD, Milne GWA, Wang S. Recognition and interaction of small rings with the ricin A-chain binding site. *Proteins* 1998; **31**: 33–41.
42. Frantz M, Jung ML, Riberau-Gayon G, Anton R. Modulation of mistletoe (*Viscum album* L.) lectins cytotoxicity by carbohydrates and serum glycoproteins. *Arzneimittelforsch/Drug Res.* 2000; **50**: 471–478.
43. Büssing A, Suzart K, Bergmann J, Pfüller U, Schietzel M, Schweizer K. Induction of apoptosis in human lymphocytes treated with *Viscum album* L. is mediated by the mistletoe lectins. *Cancer Lett.* 1996; **99**: 59–72.

